

Carbene and Isocyanide Ligation at Luminescent Cyclometalated 6-Phenyl-2,2'-bipyridyl Platinum(II) Complexes: Structural and Spectroscopic Studies

Siu-Wai Lai, Michael Chi-Wang Chan, Kung-Kai Cheung, and Chi-Ming Che*

Department of Chemistry, The University of Hong Kong, Pokfulam Road, Hong Kong

Received April 12, 1999

A series of luminescent cyclometalated platinum(II) diamino–carbene complexes, namely, $[(\text{CNN})\text{Pt}\{\text{C}(\text{NHR}^1)(\text{NHR}^2)\}]^+$ (HCNN = 6-phenyl-2,2'-bipyridine; for $\text{R}^1 = \text{tBu}$, $\text{R}^2 = \text{Me}$ (**2**), NH_2 (**3**), CH_2Ph (**4**); for $\text{R}^1 = 2,6\text{-Me}_2\text{C}_6\text{H}_3$ (Ar'), $\text{R}^2 = \text{Me}$ (**6**), NH_2 (**7**), CH_2Ph (**8**)), are synthesized by nucleophilic attack of amines at the coordinated isocyanide ligands of $[(\text{CNN})\text{PtC}\equiv\text{NR}^1]^+$ ($\text{R}^1 = \text{tBu}$ (**1**), Ar' (**5**)). The binuclear bridging bis(carbene) derivative $[(\text{CNN})\text{Pt}\{2\mu\text{-}\{\text{C}(\text{NHtBu})(\text{NH}(\text{CH}_2)_3)\}_2\text{NMe}\}]^{2+}$ (**9**) is prepared by treatment of **1** with excess 3,3'-diamino-*N*-methylpropylamine. The molecular structures of **2**(ClO_4)·0.5 H_2O , **3**(ClO_4)·0.5 H_2O , **4**(ClO_4), and **6**(ClO_4) reveal Pt–C(carbene) distances of 1.997(7), 1.992(4), 1.989(6), and 1.996(8) Å, respectively. Short N–C(carbene) bond lengths (mean 1.332 Å) imply substantial $p_\pi\text{-}p_\pi$ interactions within the N–C(carbene)–N fragment, and minimal π bonding in the Pt–C(carbene) moiety is inferred. Weak $\pi\text{-}\pi$ stacking interactions between the CNN ligands are observed in the crystal lattice of **2–4** and **6** (range 3.5–3.6 Å). Complexes **1–9** display structureless emissions, with λ_{max} ranging from 528 to 558 nm in acetonitrile at 298 K, and they are assigned to $^3\text{MLCT}$ excited states. The emissions of **1** and **5** exhibit noticeably higher quantum yields, which reflect the strong ligand field strength of the isocyanide auxiliaries. The 77 K emissions of **1–9** in frozen acetonitrile are blue-shifted and display well-resolved vibronic structures. At high concentrations ($\geq 10^{-5}$ M), **1** and **5** show an additional low-energy band at 627 (in butyronitrile) and 730 nm which are ascribed to $\pi\text{-}\pi$ excimeric and MMLCT emissions, respectively. The solid-state emissions of complexes **1**(ClO_4)–**9**(ClO_4)₂ (except **5**(ClO_4)) at 298 K are red-shifted from solution to λ_{max} 553–579 nm with a shoulder at 595–612 nm. They are tentatively assigned to $^3\text{MLCT}$ excited states with excimeric character due to weak CNN $\pi\text{-}\pi$ interactions, as evident in the crystal structures. The remarkable low-energy luminescence of **5**(ClO_4) in the solid state (λ_{max} 704 nm at 298 K; 781 nm at 77 K) is attributed to MMLCT transitions arising from solid-state intermolecular stacking interactions. Upon photolysis with UV–visible light, reaction between complex **2** and iodomethane in acetonitrile leads to decomposition of the diamino–carbene ligand and generation of the platinum(IV) diiodide cyanide derivative *trans*- $[(\text{CNN})\text{Pt}(\text{C}\equiv\text{N})\text{I}_2]$ (**10**).

Introduction

Reports regarding the generation and reactivity of platinum carbene complexes have predominantly emphasized divalent species.^{1–4} The vast majority of these

are stabilized by at least one heteroatom, and isolation of congeners without such heteroatoms is rare.⁵ Scant attention, however, has been granted to their photo-physical and photochemical properties, even though photolysis can alter their intrinsic reactivity through population of charge-transfer excited states. A pertinent example of platinum(II) photocatalysis is the prolific excited-state chemistry of $[\text{Pt}_2(\mu\text{-P}_2\text{O}_5\text{H}_2)_4]^{4-}$, which can mediate light-induced C–H and C–halogen bond activation and electron/atom transfer reactions.⁶ The first observation of a metal $\rightarrow \pi^*$ (carbene) charge transfer excited state in solution was recently published for a hexanuclear Pt(II) macrocycle with metallacyclic bis-

* Fax: (852) 2857 1586. E-mail: cmche@hkucc.hku.hk.

(1) (a) Hartley, F. R. *Comprehensive Organometallic Chemistry*; Wilkinson, G., Stone, F. G. A., Abel, E. W., Eds.; Pergamon: New York, 1982; Vol. 6, p 502. (b) Lappert, M. F. *J. Organomet. Chem.* **1988**, *358*, 185. (c) Cross, R. J. *Comprehensive Organometallic Chemistry II*; Wilkinson, G., Stone, F. G. A., Abel, E. W., Puddephatt, R. J., Eds.; Pergamon: New York, 1995; Vol. 9, p 419.

(2) Recent examples: (a) Crociani, B.; Di Bianca, F.; Fontana, A.; Forsellini, E.; Bombieri, G. *J. Chem. Soc., Dalton Trans.* **1994**, 407. (b) Zhang, S. W.; Kaharu, T.; Pirio, N.; Ishii, R.; Uno, M.; Takahashi, S. *J. Organomet. Chem.* **1995**, *489*, C62. (c) Fehlhammer, W. P.; Metzner, R.; Luger, P.; Dauter, Z. *Chem. Ber.* **1995**, *128*, 1061. (d) Michelin, R. A.; Mozzon, M.; Vialetto, B.; Bertani, R.; Benetollo, F.; Bombieri, G.; Angelici, R. *J. Organometallics* **1996**, *15*, 4096. (e) Holtcamp, M. W.; Labinger, J. A.; Bercaw, J. E. *J. Am. Chem. Soc.* **1997**, *119*, 848. (f) Kernbach, U.; Lügger, T.; Hahn, F. E.; Fehlhammer, W. P. *J. Organomet. Chem.* **1997**, *541*, 51.

(3) Pt(0) derivatives: Arduengo, A. J., III; Gamper, S. F.; Calabrese, J. C.; Davidson, F. *J. Am. Chem. Soc.* **1994**, *116*, 4391.

(4) Pt(IV) derivatives: (a) Rendina, L. M.; Vittal, J. J.; Puddephatt, R. J. *Organometallics* **1995**, *14*, 1030, and references therein. (b) Zhang, S. W.; Takahashi, S. *Organometallics* **1998**, *17*, 4757.

(5) (a) Lu, Z.; Jones, W. M.; Winchester, W. R. *Organometallics* **1993**, *12*, 1344. (b) Cave, G. W. V.; Hallett, A. J.; Errington, W.; Rourke, J. P. *Angew. Chem., Int. Ed.* **1998**, *37*, 3270.

(6) Roundhill, D. M.; Gray, H. B.; Che, C. M. *Acc. Chem. Res.* **1989**, *22*, 55.

(carbene) ligands,⁷ and accounts of luminophores bearing aminocarbene groups have also appeared.⁸ The photochemistry of pentacarbonyl tungsten and chromium Fischer carbene complexes has been extensively studied.^{9,10}

We and other researchers have been engaged in the development of cyclometalated Pt(II) derivatives containing substituted pyridyl and 2,2'-bipyridyl ligands from a photochemical perspective.^{11–14} In particular, complexes derived from 6-phenyl-2,2'-bipyridine (HCNN) display low-lying metal-to-ligand charge transfer (MLCT) excited states which generally exhibit improved photophysical properties compared to 2,2':6',2''-terpyridine (tpy) analogues.^{15,16} We now present the preparation, molecular structures, and photophysical properties of a series of cyclometalated platinum(II) diamino-carbene complexes and the corresponding isocyanide precursors. All new derivatives are photoluminescent at room temperature in fluid solution. In addition, isolation of a binuclear Pt(II) complex supported by an unusual bidentate bis(carbene) bridge and the photochemical reactivity of the carbene complexes with iodomethane are described.

Experimental Section

General Procedures. All starting materials were used as received from commercial sources. 6-Phenyl-2,2'-bipyridine (HCNN)¹⁷ and [(CNN)PtCl]¹⁵ were prepared by literature methods. (**Caution:** perchlorate salts are potentially explosive and should be handled with care and in small amounts.) Acetonitrile for photophysical measurements was distilled over potassium permanganate and calcium hydride. All other solvents were of analytical grade and purified according to conventional methods.¹⁸

Fast atom bombardment (FAB) mass spectra were obtained on a Finnigan Mat 95 mass spectrometer. ¹H (300 MHz) and ¹³C (126 MHz) spectra were recorded on DPX 300 and 500 Bruker FT-NMR spectrometers respectively with chemical shifts (in ppm) relative to tetramethylsilane. Due to restricted rotation about the C(carbene)–N bonds, multiple peaks for each amino substituent are typically observed by NMR spectroscopy. In the ¹³C NMR spectra, all resolved peaks for aliphatic carbons are recorded, while only the most intense signals for aryl carbons are given. Elemental analysis was performed by the Institute of Chemistry at the Chinese

Academy of Sciences, Beijing. Infrared spectra were recorded in Nujol on a BIO RAD FT-IR spectrometer. UV–vis spectra were recorded on a Perkin-Elmer Lambda 19 UV/vis spectrophotometer.

Emission and Lifetime Measurements. Steady-state emission spectra were recorded on a SPEX 1681 Fluorolog-2 series F111AI spectrophotometer. Low-temperature (77 K) emission spectra for glasses and solid-state samples were recorded in 5 mm diameter quartz tubes which were placed in a liquid nitrogen Dewar equipped with quartz windows. The emission spectra were corrected for monochromator and photomultiplier efficiency and for xenon lamp stability.

Sample and standard solutions were degassed with at least three freeze–pump–thaw cycles. The emission quantum yield was measured by the method of Demas and Crosby¹⁹ with [Ru(bpy)₃](PF₆)₂ in degassed acetonitrile as the standard ($\Phi_r = 0.062$) and calculated by $\Phi_s = \Phi_r(B_r/B_s)(n_s/n_r)^2(D_s/D_r)$, where the subscripts s and r refer to sample and reference standard solution respectively, n is the refractive index of the solvents, D is the integrated intensity, and Φ is the luminescence quantum yield. The quantity B is calculated by $B = 1 - 10^{-AL}$, where A is the absorbance at the excitation wavelength and L is the optical path length.

Emission lifetime measurements were performed with a Quanta Ray DCR-3 pulsed Nd:YAG laser system (pulse output 355 nm, 8 ns). The emission signals were detected by a Hamamatsu R928 photomultiplier tube and recorded on a Tektronix model 2430 digital oscilloscope. Errors for λ values (± 1 nm), τ ($\pm 10\%$), and ϕ ($\pm 10\%$) are estimated.

Synthesis. [(CNN)Pt(C≡N^tBu)]ClO₄, **1**(ClO₄). To an orange suspension of [(CNN)PtCl] (0.10 g, 0.22 mmol) in acetonitrile (20 mL) at room temperature was added excess *tert*-butylisocyanide, ^tBuN≡C (0.5 mL, 4.4 mmol). Upon stirring, the color of the mixture changed to cloudy orange-red, then clear pale yellow after 30 min. Addition of excess LiClO₄ in acetonitrile followed by diethyl ether yielded a yellow precipitate, which was collected and dried. Recrystallization by slow diffusion of diethyl ether into an acetonitrile solution of the crude product afforded yellow crystals: yield 0.12 g, 91%. Anal. Calcd for C₂₁H₂₀N₃O₄ClPt: C, 41.42; H, 3.31; N, 6.90. Found: C, 41.65; H, 3.06; N, 6.62. FAB-MS: m/z 509 [M⁺], 426 [M⁺ – C≡N^tBu]. ¹H NMR (CD₃CN): 1.73 (s, 9H, ^tBu), 7.14 (m, 3H), 7.43 (m, 1H), 7.72 (m, 2H), 7.83 (d, 1H, $J = 7.8$ Hz), 8.02 (t, 1H, $J = 8.0$ Hz), 8.11 (d, 1H, $J = 7.9$ Hz), 8.25 (t, 1H, $J = 7.9$ Hz), 8.57 (d, 1H, $J = 5.1$ Hz). ¹³C{¹H} NMR (CD₃CN): 30.2 (CMe₃), 61.5 (CMe₃), 121.0, 121.4, 125.6, 127.0, 127.2, 130.3, 133.3, 138.1, 138.3, 142.6, 144.0, 148.0, 153.8, 156.2, 157.8, 165.9, Pt–CN^tBu not resolved. IR (Nujol): $\nu = 2207$ (C≡N), 1603 (C=N) cm⁻¹.

[(CNN)Pt{C(NH^tBu)(NHMe)}]ClO₄, **2**(ClO₄). A stirred solution of **1**(ClO₄) (0.10 g, 0.16 mmol) in acetonitrile (20 mL) and excess MeNH₂ (40 wt % solution in water, 0.5 mL, 5.8 mmol) was heated at reflux for 24 h. After cooling, the volume of solution was reduced to ~5 mL, and addition of excess LiClO₄ in acetonitrile gave an orange solid, which was collected by filtration and dried. Recrystallization by slow diffusion of diethyl ether into an acetonitrile solution yielded orange crystals: yield 0.08 g, 76%. Anal. Calcd for C₂₂H₂₅N₄O₄ClPt: C, 41.29; H, 3.94; N, 8.75. Found: C, 41.21; H, 4.26; N, 8.96. FAB-MS: m/z 540 [M⁺], 481 [M⁺ – ^tBu]. ¹H NMR (CD₃CN): 1.45, 1.50, 1.53 (3 singlets, 9H, ^tBu), 2.95, 3.19, 3.27 (3 doublets, 3H, ³J_{HH} = 4.8 Hz, NMe), 7.14 (m, 3H), 7.58 (m, 1H), 7.63 (m, 1H), 7.87 (m, 1H), 7.97 (m, 1H), 8.09 (m, 1H), 8.23 (m, 2H), 8.57 (m, 1H). ¹³C{¹H} NMR (CD₃CN): 29.5, 31.8, 31.9 (CMe₃), 36.9, 37.1, 37.2 (NMe), 54.6, 54.8, 55.3 (CMe₃), 120.4, 120.6, 125.2, 125.6, 126.2, 129.6, 132.4, 138.1, 138.6, 141.7, 142.3, 148.2, 153.5, 155.3, 159.0, 165.1, 193.7 (Pt–C_{carbene}, ¹J_{PtC} = 1363 Hz). IR (Nujol): $\nu = 3383$ (br, N–H), 1599, 1552 (C=N) cm⁻¹.}}

(19) Demas, J. N.; Crosby, G. A. *J. Phys. Chem.* **1971**, *75*, 991.

(7) Lai, S. W.; Cheung, K. K.; Chan, M. C. W.; Che, C. M. *Angew. Chem., Int. Ed.* **1998**, *37*, 182.

(8) (a) Xue, W. M.; Chan, M. C. W.; Su, Z. M.; Cheung, K. K.; Liu, S. T.; Che, C. M. *Organometallics* **1998**, *17*, 1622. (b) Yam, V. W. W.; Chu, B. W. K.; Cheung, K. K. *Chem. Commun.* **1998**, 2261.

(9) Hegedus, L. S. *Acc. Chem. Res.* **1995**, *28*, 299.

(10) (a) Foley, H. C.; Strubinger, L. M.; Targos, T. S.; Geoffroy, G. L. *J. Am. Chem. Soc.* **1983**, *105*, 3064. (b) Bell, S. E. J.; Gordon, K. C.; McGarvey, J. J. *J. Am. Chem. Soc.* **1988**, *110*, 3107.

(11) (a) Chassot, L.; Müller, E.; von Zelewsky, A. *Inorg. Chem.* **1984**, *23*, 4249. (b) Sandrini, D.; Maestri, M.; Balzani, V.; Chassot, L.; von Zelewsky, A. *J. Am. Chem. Soc.* **1987**, *109*, 7720.

(12) (a) Chan, C. W.; Lai, T. F.; Che, C. M.; Peng, S. M. *J. Am. Chem. Soc.* **1993**, *115*, 11245. (b) Chan, C. W.; Cheng, L. K.; Che, C. M. *Coord. Chem. Rev.* **1994**, *132*, 87.

(13) Tse, M. C.; Cheung, K. K.; Chan, M. C. W.; Che, C. M. *Chem. Commun.* **1998**, 2295.

(14) (a) Zheng, G. Y.; Rillema, D. P.; DePriest, J.; Woods, C. *Inorg. Chem.* **1998**, *37*, 3588. (b) Zheng, G. Y.; Rillema, D. P. *Inorg. Chem.* **1998**, *37*, 1392.

(15) Cheung, T. C.; Cheung, K. K.; Peng, S. M.; Che, C. M. *J. Chem. Soc., Dalton Trans.* **1996**, 1645.

(16) Lai, S. W.; Chan, M. C. W.; Cheung, T. C.; Peng, S. M.; Che, C. M. *Inorg. Chem.*, in press.

(17) Kröhnke, F. *Synthesis* **1976**, 1.

(18) Perrin, D. D.; Armarego, W. L. F.; Perrin, D. R. *Purification of Laboratory Chemicals*, 2nd ed.; Pergamon: Oxford, 1980.

[(CNN)Pt{C(NH^tBu)(NHNH₂)}]ClO₄, **3(ClO₄).** The procedure for **2**(ClO₄) was adopted using excess hydrazine hydrate (0.3 mL, 9.6 mmol) to afford an orange crystalline solid: yield 0.07 g, 67%. Anal. Calcd for C₂₁H₂₄N₅O₄ClPt: C, 39.35; H, 3.77; N, 10.93. Found: C, 39.44; H, 3.58; N, 10.68. FAB-MS: *m/z* 540 [M⁺]. ¹H NMR (CD₃CN): 1.50 (s, 9H, ^tBu), 4.01 (s, 2H, NH₂), 7.16 (m, 2H), 7.58 (m, 1H), 7.68 (m, 1H), 7.86 (m, 1H), 7.96 (m, 2H), 8.09 (m, 1H), 8.25 (m, 2H), 8.57 (m, 1H). ¹³C{¹H} NMR (CD₃CN): 31.6 (CMe₃), 53.6 (CMe₃), 120.2, 120.5, 125.1, 125.5, 126.1, 129.4, 132.2, 138.4, 141.5, 141.9, 142.5, 148.1, 153.2, 155.1, 158.8, 164.9, 185.2 (Pt–C_{carbene}, ¹J_{PtC} = 1274 Hz). IR (Nujol): ν = 3369, 3291 (N–H), 1597, 1540 (C=N) cm⁻¹.

[(CNN)Pt{C(NH^tBu)(NHCH₂Ph)}]ClO₄, **4(ClO₄).** The procedure for **2**(ClO₄) was adopted using excess benzylamine (0.5 mL, 4.6 mmol) to afford orange crystals: yield 0.09 g, 77%. Anal. Calcd for C₂₈H₂₉N₄O₄ClPt: C, 46.96; H, 4.08; N, 7.82. Found: C, 47.10; H, 4.17; N, 7.93. FAB-MS: *m/z* 616 [M⁺]. ¹H NMR (CD₃CN): 1.42, 1.45, 1.55 (3 singlets, 9H, ^tBu), 4.53–5.05 (m, 2H, NCH₂), 7.01 (m, 2H), 7.18 (m, 5H), 7.45 (m, 2H), 7.60 (m, 1H), 7.88 (m, 2H), 8.09 (m, 4H). ¹³C{¹H} NMR (CD₃CN): 29.4, 31.7 (CMe₃), 53.7 (NCH₂), 54.8, 55.0 (CMe₃), 120.3, 120.6, 124.8, 125.7, 126.3, 128.3, 128.9, 129.2, 132.5, 137.1, 138.2, 140.4, 141.1, 142.3, 148.1, 152.7, 153.6, 155.1, 158.4, 164.7, 194.0 (Pt–C_{carbene}). IR (Nujol): ν = 3388, 3313 (N–H), 1599, 1551 (C=N) cm⁻¹.

[(CNN)PtC≡NAr']ClO₄, **5(ClO₄).** To an orange suspension of [(CNN)PtCl] (0.10 g, 0.22 mmol) in acetonitrile (20 mL) was added 2,6-dimethylphenyl (Ar') isocyanide (0.03 g, 0.23 mmol). The mixture was stirred for 10 min to yield a purple precipitate and yellow solution. After addition of excess LiClO₄ in acetonitrile followed by diethyl ether, the resultant purple solid was collected and dried. Recrystallization by slow diffusion of diethyl ether into an acetonitrile solution afforded a purple crystalline solid: yield 0.11 g, 77%. Anal. Calcd for C₂₅H₂₀N₃O₄ClPt: C, 45.70; H, 3.07; N, 6.40. Found: C, 45.84; H, 3.06; N, 6.26. FAB-MS: *m/z* 555 [M⁺], 423 [M⁺ – CNAr']. ¹H NMR (CD₃CN): 2.56 (s, 6H, Me), 7.15 (m, 2H), 7.32 (d, 2H, *J* = 7.5 Hz), 7.43 (m, 2H), 7.52 (m, 1H), 7.74 (m, 1H), 7.82 (d, 1H, *J* = 8.2 Hz), 7.93 (d, 1H, *J* = 8.0 Hz), 8.09 (m, 1H), 8.24 (m, 2H), 8.80 (d, 1H, *J* = 5.6 Hz). The poor solubility of **5**(ClO₄) in common deuterated solvents precluded its characterization by ¹³C NMR spectrum. IR (Nujol): ν = 2169 (C≡N), 1603 (C=N) cm⁻¹.

[(CNN)Pt{C(NHAr')(NHMe)}]ClO₄, **6(ClO₄).** The procedure for **2**(ClO₄) was adopted using **5**(ClO₄) (0.10 g, 0.15 mmol) and excess MeNH₂ (40 wt % solution in water, 0.5 mL, 5.8 mmol) to yield orange crystals: yield 0.07 g, 67%. Anal. Calcd for C₂₆H₂₅N₄O₄ClPt: C, 45.39; H, 3.66; N, 8.14. Found: C, 45.65; H, 3.58; N, 7.82. FAB-MS: *m/z* 588 [M⁺]. ¹H NMR (CD₃CN): 2.38, 2.40 (2 singlets, 6H, Me₂C₆H₃), 3.17 (d, 3H, *J* = 4.7 Hz, NMe), 6.82 (s with ¹⁹⁵Pt satellites, 1H, ³J_{PtH} = 91 Hz, NH), 7.19 (m, 2H), 7.28 (m, 3H), 7.36 (d, 1H, *J* = 7.2 Hz), 7.63 (d, 1H, *J* = 6.9 Hz), 7.76 (m, 1H), 7.89 (d, 1H, *J* = 8.1 Hz), 7.99 (d, 1H, *J* = 8.0 Hz), 8.11 (t, 1H, *J* = 8.0 Hz), 8.28 (m, 2H), 8.75 (d, 1H, *J* = 5.2 Hz). ¹³C{¹H} NMR (CD₃CN): 19.1, 19.3 (Me₂C₆H₃), 36.3 (NMe), 120.5, 120.7, 125.6, 126.1, 126.6, 129.7, 129.9, 130.2, 130.3, 132.4, 134.7, 137.3, 137.6, 137.9, 139.9, 141.9, 142.5, 148.5, 153.0, 155.1, 158.9, 164.9, 188.4 (Pt–C_{carbene}, ¹J_{PtC} = 1321 Hz). IR (Nujol): ν = 3336, 3300 (N–H), 1600, 1552 (C=N) cm⁻¹.

[(CNN)Pt{C(NHAr')(NHNH₂)}]ClO₄, **7(ClO₄).** The procedure for **6**(ClO₄) was adopted using excess hydrazine hydrate (0.3 mL, 9.6 mmol) to afford an orange-red crystalline solid: yield 0.06 g, 57%. Anal. Calcd for C₂₅H₂₄N₅O₄ClPt: C, 43.58; H, 3.51; N, 10.16. Found: C, 43.48; H, 3.33; N, 10.28. FAB-MS: *m/z* 589 [M⁺]. ¹H NMR (CD₃CN): 2.39, 2.40 (2 singlets, 6H, Me), 4.38 (broad s, 2H, NH₂), 6.88 (m, 3H), 6.99 (m, 2H), 7.08 (m, 1H), 7.26 (m, 2H), 7.55 (d, 1H, *J* = 8.0 Hz), 7.67 (d, 1H, *J* = 7.8 Hz), 7.88 (m, 2H), 8.08 (m, 1H), 8.47 (d, 1H, *J* = 4.6 Hz), 8.63 (broad s, 1H, NH), 9.72 (s with ¹⁹⁵Pt satellites,

1H, ³J_{PtH} = 92 Hz, NH). ¹³C{¹H} NMR (CD₃CN): 19.9 (Me), 120.1, 120.4, 125.0, 125.6, 126.2, 127.9, 128.9, 129.2, 131.7, 132.3, 135.9, 138.1, 141.4, 142.1, 147.9, 153.0, 154.9, 158.4, 164.7, 187.0 (Pt–C_{carbene}). IR (Nujol): ν = 3320 (br, N–H), 1603, 1555 (C=N) cm⁻¹.

[(CNN)Pt{C(NHAr')(NHCH₂Ph)}]ClO₄, **8(ClO₄).** The procedure for **6**(ClO₄) was adopted using excess benzylamine (0.5 mL, 4.6 mmol) to afford orange crystals: yield 0.08 g, 69%. Anal. Calcd for C₃₂H₂₉N₄O₄ClPt: C, 50.30; H, 3.83; N, 7.33. Found: C, 50.15; H, 3.98; N, 7.48. FAB-MS: *m/z* 664 [M⁺]. ¹H NMR (CD₃CN): 2.37, 2.39 (2 singlets, 6H, Me), 4.67 (dd, 1H, ²J_{HH} = 14.8 Hz, ³J_{HH} = 6.1 Hz, NCH₂), 4.88 (dd, 1H, ²J_{HH} = 14.8 Hz, ³J_{HH} = 6.1 Hz, NCH₂), 7.06 (d, 2H, *J* = 6.5 Hz), 7.18–7.32 (m, 7H), 7.42 (m, 1H), 7.58 (m, 2H), 7.89 (d, 1H, *J* = 8.1 Hz), 7.96 (d, 1H, *J* = 7.7 Hz), 8.09 (t, 1H, *J* = 8.0 Hz), 8.21 (m, 2H), 8.32 (d, 1H, *J* = 5.3 Hz), 8.55 (broad s, 1H, NH). ¹³C{¹H} NMR (CD₃CN): 19.1, 19.3 (Me), 53.0 (NCH₂), 120.4, 120.7, 125.3, 126.1, 126.6, 128.5, 129.1, 129.2, 129.5, 130.0, 130.3, 130.4, 132.4, 134.7, 137.1, 137.6, 137.8, 140.0, 140.1, 141.5, 142.5, 148.6, 152.8, 155.2, 158.6, 164.9, 189.4 (Pt–C_{carbene}). IR (Nujol): ν = 3340, 3264 (N–H), 1601, 1540 (C=N) cm⁻¹.

[(CNN)Pt]₂μ-{C(NH^tBu)(NH(CH₂)₃)}₂NMe](ClO₄)₂, **9(ClO₄)₂.** A solution of **1**(ClO₄) (0.10 g, 0.16 mmol) and excess 3,3'-diamino-*N*-methylpropylamine (CH₃N(CH₂CH₂CH₂NH₂)₂) (0.1 mL, 0.62 mmol) in acetonitrile (20 mL) was heated at reflux for 12 h. Upon cooling, the solution volume was reduced, and addition of diethyl ether yielded an oily yellow solid, which was washed repeatedly with *n*-hexane. Recrystallization by slow diffusion of *n*-pentane into a CH₂Cl₂ solution afforded a yellow solid: yield 0.07 g, 63%. FAB-MS: *m/z* (%) = 1264 [M⁺ + ClO₄]. Anal. Calcd for C₄₉H₅₉N₉O₈Cl₂Pt₂: C, 43.18; H, 4.36; N, 9.25. Found: C, 43.39; H, 4.13; N, 9.09. ¹H NMR (CD₃CN): 1.37–1.53 (m, CMe₃), 1.7–3.8 (m, triamine), 7.14, 7.44–7.75, 7.86, 8.00, 8.09, 8.24, 8.59 (m, aryl H). ¹³C{¹H} NMR (CD₃CN): 28.6–31.7 (CMe₃, triamine), 47.5–48.0, 54.6–55.1 (CMe₃, triamine), 120.5–120.7, 125.3–127.2, 129.9–130.3, 132.5–133.2, 138.1–138.5, 141.7–144.0, 148.2, 152.8–155.2, 164.6, 172.0, 192.6 (Pt–C_{carbene}). IR (Nujol): ν = 3384 (br, N–H), 1630, 1568 (C=N) cm⁻¹.

trans-[(CNN)Pt(C≡N)I₂], **10.** A solution of **2**(ClO₄) (0.10 g, 0.16 mmol) in dried and degassed acetonitrile (20 mL) containing iodomethane (10 mL) was irradiated with UV-visible light (RPR-100 Rayonet photochemical chamber reactor equipped with 16 8-W RPR 3500 Å Hg lamps) for 12 h at room temperature. An orange precipitate was obtained and collected by filtration. Slow evaporation of a methanol/dimethylformamide (v/v 1:1) solution of the crude product afforded orange crystals: yield 0.08 g, 73%. Anal. Calcd for C₁₇H₁₁N₃I₂Pt: C, 28.91; H, 1.57; N, 5.95. Found: C, 28.99; H, 1.70; N, 5.74. FAB-MS: *m/z* 707 [M⁺]. ¹H NMR (DMSO-*d*₆): 7.15 (m, 1H), 7.42 (d, 1H, *J* = 6.3 Hz), 7.50 (d, 1H, *J* = 7.3 Hz), 7.99 (m, 1H), 8.07 (d, 1H, *J* = 7.4 Hz), 8.50 (m, 3H), 8.65 (d, 1H, *J* = 7.0 Hz), 8.90 (d, 1H, *J* = 7.7 Hz), 9.03 (m, 1H). ¹³C{¹H} NMR (DMSO-*d*₆): 87.5 (C≡N), 122.1, 122.2, 123.4, 125.9, 126.2, 126.9, 129.3, 133.0, 136.2, 141.8, 142.8, 144.6, 151.6, 151.9, 155.7, 161.3. IR (Nujol): ν = 2155 (C≡N), 1598 (C=N) cm⁻¹.

X-ray Crystallography. Crystals of **2**(ClO₄)·0.5H₂O (see Supporting Information for all data), **3**(ClO₄)·0.5H₂O, **4**(ClO₄), and **6**(ClO₄) were grown by slow diffusion of diethyl ether into acetonitrile solutions. Crystals of **10** were obtained by slow evaporation of methanol/dimethylformamide solution. Crystal data and details of collection and refinement are summarized in Table 1.

Diffraction experiments were performed at 301 K on a Rigaku AFC7R (**2**(ClO₄)·0.5H₂O and **4**(ClO₄)) or Nonius-Enraf (**3**(ClO₄)·0.5H₂O) diffractometer with graphite-monochromatized Mo K α radiation (λ = 0.71073 Å) using ω - 2θ scans. For **6**(ClO₄) and **10**, intensity data were collected on a MAR diffractometer with graphite-monochromatized Mo K α radiation (λ = 0.71073 Å) using a 300 mm image plate detector.

For **2**(ClO₄)·0.5H₂O, **3**(ClO₄)·0.5H₂O, **4**(ClO₄), and **10**, the

Table 1. Crystal Data

	3 (ClO ₄)·0.5H ₂ O	4 (ClO ₄)	6 (ClO ₄)	10
formula	C ₂₁ H ₂₅ N ₅ O _{4.5} ClPt	C ₂₈ H ₂₉ N ₄ O ₄ ClPt	C ₂₆ H ₂₅ N ₄ O ₄ ClPt	C ₁₇ H ₁₁ N ₃ I ₂ Pt
fw	650.00	716.10	688.05	706.19
color	yellow	orange	yellow	red
crystal size, mm	0.25 × 0.10 × 0.30	0.30 × 0.10 × 0.07	0.25 × 0.20 × 0.40	0.25 × 0.15 × 0.10
crystal system	triclinic	triclinic	orthorhombic	monoclinic
space group	<i>P</i> $\bar{1}$ (No. 2)	<i>P</i> $\bar{1}$ (No. 2)	<i>Pbca</i> (No. 61)	<i>P2</i> ₁ / <i>c</i> (No. 14)
<i>a</i> , Å	11.866(4)	11.070(2)	8.758(2)	9.080(2)
<i>b</i> , Å	13.102(5)	11.216(2)	21.560(3)	22.843(3)
<i>c</i> , Å	8.392(2)	13.065(3)	26.533(3)	9.291(2)
α , deg	100.30(3)	111.29(1)		
β , deg	97.50(4)	106.97(1)		116.43(2)
γ , deg	72.88(3)	101.67(1)		
<i>V</i> , Å ³	1222.6(8)	1356(1)	5010(1)	1725.7(6)
<i>Z</i>	2	2	8	4
<i>D</i> _c (g cm ⁻³)	1.766	1.753	1.824	2.718
μ , cm ⁻¹	58.63	52.91	57.26	116.80
<i>F</i> (000)	634	704	2688	1272
2 θ _{max} , deg	50	50	51	51
no. unique data	4272	4786	4799	3172
no. obsd data for <i>I</i> > 3 σ (<i>I</i>)	3852	3957	2876	2549
no. variables	307	345	331	198
<i>R</i> ^a	0.022	0.029	0.037	0.031
<i>R</i> _w ^b	0.028	0.037	0.046	0.043
residual ρ , e Å ⁻³	+0.85, -0.59	+0.90, -0.71	+0.86, -1.47	+1.03, -1.49

$$^a R = \sum ||F_o| - |F_c|| / \sum |F_o|. \quad ^b R_w = [\sum w(|F_o| - |F_c|)^2 / \sum w|F_o|^2]^{1/2}.$$

structures were solved by Patterson and Fourier methods (*PATY*)^{20a} and refined by full-matrix least-squares using the software package *TeXsan*²¹ on a Silicon Graphics Indy computer. For **2**(ClO₄)·0.5H₂O, all 33 non-H atoms were refined anisotropically. The H atoms bonded to N(3) and N(4) were located in the difference Fourier synthesis, and their positional parameters were refined. The O atom of the water molecule is at special position, and the H atoms were not located. The remaining 23 H atoms of the complex cation at calculated positions with thermal parameters equal to 1.3 times that of the attached C atoms were not refined. For **3**(ClO₄)·0.5H₂O, all 33 non-H atoms were refined anisotropically. The 4 H atoms bonded to N(3), N(4), and N(5) were located in the difference Fourier synthesis, and their positional parameters were refined. The O atom of the water molecule is at special position, and the H atoms bonded to it were not located. Twenty H atoms at calculated positions were not refined. For **4**(ClO₄), there is positional disorder in N(2) and C(1), and C(1') and N(2') were placed in the same sites and all four atoms were given occupancy of 0.5. The O atoms of the perchlorate anion were also disordered. In the least-squares refinement, 32 non-H atoms were refined anisotropically, N(2) and C(1) were refined isotropically, and C(1') and N(2') constrained to N(2) and C(1), respectively, were not refined. The positional parameters of H(1) and H(4) located in the difference Fourier synthesis were refined, and 25 other H atoms at calculated positions were not refined. For **10**, there is positional disorder in N(2) and C(1), and C(1') and N(2') were placed in the same sites and all four atoms were given occupancy of 0.5. In the least-squares refinement, C(1') and N(2') were constrained respectively to N(2) and C(1), which were refined isotropically, while the other 21 non-H atoms were refined anisotropically. The other 11 H atoms at calculated positions were not refined.

For **6**(ClO₄), the structures were solved by direct methods (*SIR92*),^{20b} expanded by Fourier methods, and refined by full-matrix least-squares using the software package *TeXsan* on a

Silicon Graphics Indy computer. All 36 non-H atoms were refined anisotropically. The H atoms bonded to N(3) and N(4) were located in difference Fourier synthesis, and their positional parameters were refined. The other 23 H atoms at calculated positions were not refined.

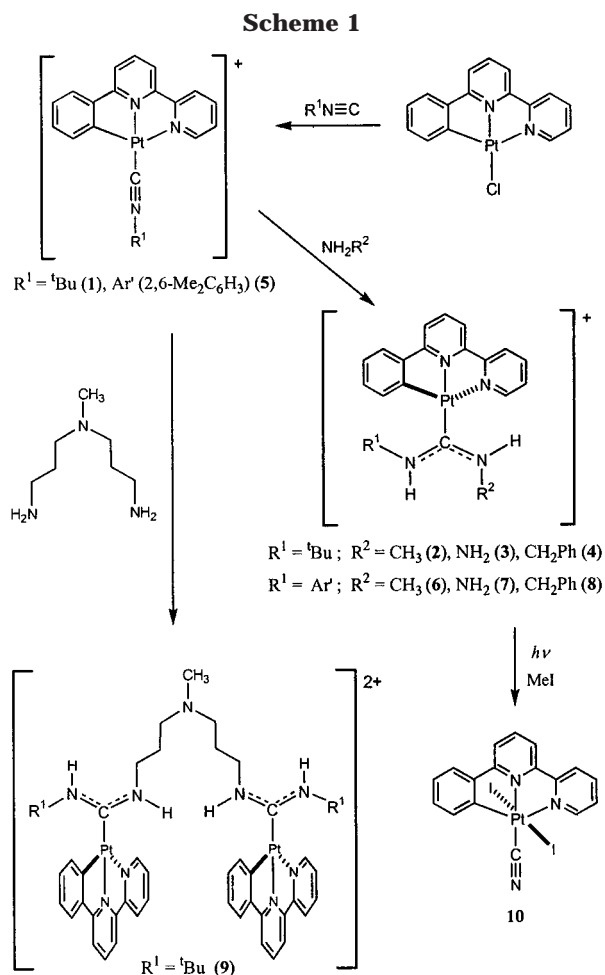
Results and Discussion

Synthesis and Characterization. The facile displacement of the chloride group from [(CNN)PtCl] by excess *tert*-butyl and 2,6-dimethylphenyl (Ar') isocyanide yielded complexes **1** and **5** as yellow and purple solids, respectively. The unusual color of the latter is discussed below. Treatment of **1** and **5** with excess amine or hydrazine afforded the diamino-carbene complexes **2–4** and **6–8** in moderate to high yields (Scheme 1). All complexes are air- and moisture-stable at room temperature. Generation of diamino-carbene derivatives has been dominated by nucleophilic attack of amines at coordinated isocyanides for decades.²² By employing this methodology using 3,3'-diamino-*N*-methylpropylamine with two isolated amine functionalities, we have prepared the binuclear species **9**, with the bidentate bis(carbene) moiety acting as a bridging ligand (Scheme 1). The FAB mass spectrum of **9** reveals a cluster around *m/z* 1264, the intensities of which are comparable to the calculated isotope pattern of [M⁺ + ClO₄] (Figure 1). We have unsuccessfully attempted analogous experiments using aliphatic and aromatic diamines (H₂N(CH₂)_{*n*}NH₂ (*n* = 2, 4), 1,4-diaminocyclohexane, 9,10-diaminophenanthrene) where intractable oily solids were afforded, while no reaction proceeded upon treatment of the carbene complexes **3** and **7** (bearing NH₂ groups) with corresponding isocyanide derivatives. Although this synthetic route is presently limited, we envisage that the bridging bidentate bis(carbene) motif will become an important ligand in the coordination chemistry of binuclear complexes.^{23a,b} A

(20) (a) *PATY*: Beurskens, P. R.; Admiraal, G.; Bosman, W. P.; Garcia-Granda, S.; Gould, R. O.; Smits, J. M. M.; Smykalla, C. The *DIREX* program system, Technical Report of the Crystallography Laboratory; University of Nijmegen: The Netherlands, 1992. (b) *SIR92*: Altomare, A.; Cascarano, M.; Giacovazzo, C.; Guagliardi, A.; Burla, M. C.; Polidori, G.; Camalli, M. *J. Appl. Crystallogr.* **1994**, *27*, 435.

(21) *TeXsan*: Crystal Structure Analysis Package; Molecular Structure Corporation, 1985 and 1992.

(22) (a) Badley, E. M.; Chatt, J.; Richards, R. L.; Sim, G. A. *J. Chem. Soc., Chem. Commun.* **1969**, 1322. (b) Belluco, U.; Crociani, B.; Michelin, R.; Uguagliati, P. *Pure Appl. Chem.* **1983**, *55*, 47.



tris(carbene) ligand generated by trialkylation followed by deprotonation of tris(imidazolyl) borate and its chelation at an Fe(III) center was recently reported.^{23c}

The characteristic IR absorptions for the isocyanide complexes **1** and **5** ($\nu(\text{C}\equiv\text{N})$ 2207 and 2169 cm^{-1} , respectively) disappear upon transformation to carbene derivatives. For the latter, broad $\nu(\text{N}-\text{H})$ bands at 3390–3260 cm^{-1} and multiple moderately intense $\nu(\text{CN})$ absorptions in the 1630–1540 cm^{-1} region are observed. The ^1H NMR spectra of the carbene compounds indicate restricted rotation about the N–C(carbene) bonds, which is typical for aminocarbene species. For example, the spectrum of **2** in CD_3CN contains three singlets at 1.45, 1.50, and 1.53 ppm ($t\text{Bu}$) and three doublets at 2.95, 3.19, and 3.27 ppm ($^3J_{\text{HH}}$ 4.8 Hz, NMe). In the ^1H NMR spectrum of **7**, two singlets at 2.39 and 2.40 ppm ($\text{Me}_2\text{C}_6\text{H}_3$) are observed, but only one broad resonance at 4.38 ppm (NH_2) is resolved due to peak broadening by the quadrupolar ^{14}N nuclei. The spectrum of **8** clearly demonstrates that the methylene hydrogens in the benzylamine moiety are diastereotopic: two doublet of doublets are observed at 4.67 and 4.88 ppm ($^2J_{\text{HH}}$ 14.8 Hz, $^3J_{\text{HH}}$ 6.1 Hz).

In the ^{13}C NMR spectra, the carbene resonances for **2–4** and **6–8** (185.2–194.0 ppm), with attendant ^{195}Pt satellites ($^1J_{\text{PtC}}$ 1274–1363 Hz), are upfield from typical

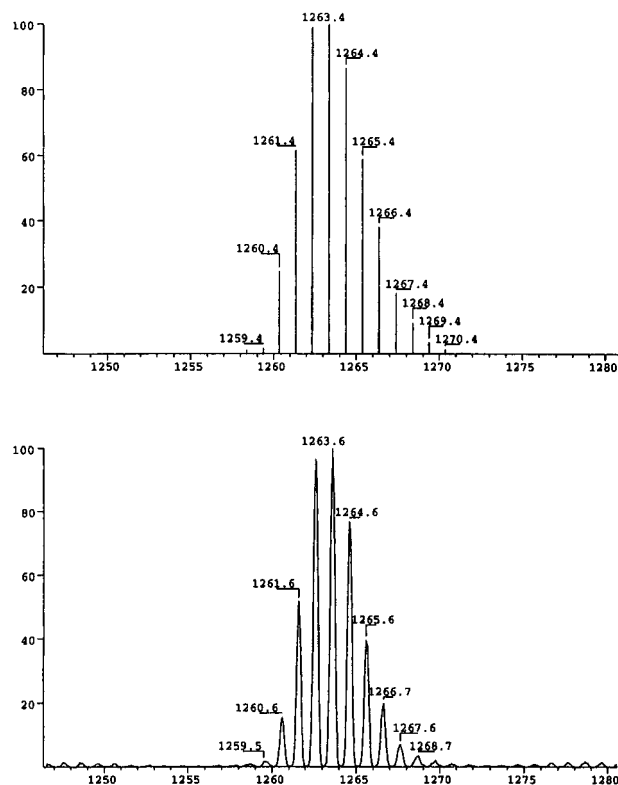


Figure 1. Calculated (top) and experimental (bottom) isotopic distribution pattern of $[\text{M}^+ + \text{ClO}_4^-]$ for **9**.

Fischer carbene complexes.²⁴ They are nevertheless comparable with Pt(II) analogues, e.g., *trans*- $[\text{PtCl}_2(\text{P}^n\text{Bu}_3)\{\text{C}(\text{NMeCH}_2)_2\}]$ (196.5 ppm in $\text{CDCl}_3/\text{C}_6\text{F}_6$)²⁵ and $[\text{PtH}\{\text{C}(\text{NCH}_2\text{CH}_2\text{CH}_2)\text{NH-}p\text{-MeOC}_6\text{H}_4\}\{\text{dppe}\}]\text{BF}_4$ (194.5 ppm in CD_2Cl_2),²⁶ and Pt(IV) congeners, e.g., $[\text{PtClMe}_2(\text{CCINMe}_2)(4,4'\text{-}t\text{Bu}_2\text{bpy})]\text{Cl}$ (171.3 ppm in CD_2Cl_2)^{4a} and $\text{PtI}_2\{\text{C}(\text{NHPr})\text{NH-}3,4\text{-(OMe)}_2\text{C}_6\text{H}_2\}_2$ (185.2 ppm in acetone- d_6).^{4b} The carbene $^1J_{\text{PtC}}$ values are characteristic for cationic Pt(II) diamino–carbene derivatives such as $[\text{PtH}\{\text{C}(\text{NCH}_2\text{CH}_2\text{CH}_2)\text{NH-}p\text{-MeOC}_6\text{H}_4\}\{\text{dppe}\}]\text{BF}_4$ (1134 Hz in CD_2Cl_2),²⁵ but are also surprisingly similar to that for the Pt(IV) species $[\text{PtClMe}_2(\text{CCINMe}_2)(4,4'\text{-}t\text{Bu}_2\text{bpy})]\text{Cl}$ (1325 Hz in CD_2Cl_2).^{4a}

Photochemical Reactivity. A prominent characteristic of square-planar platinum(II) complexes is their ability to undergo oxidative addition reactions which are markedly dependent on the nature of ancillary ligands. The platinum(II) diamino–carbene complexes in this work are relatively unreactive in comparison with Fischer carbene complexes of the early transition metals.^{1,24} Nevertheless, a photochemical reaction was observed when a degassed acetonitrile solution of **2** containing iodomethane was exposed to UV radiation for 12 h at room temperature. The reaction was monitored by UV–vis spectroscopy, which depicted a gradual decrease in absorbance at λ_{max} 336 and 350 nm accompanied by growth of a band at λ_{max} 367 nm. The new band corresponds to the Pt(IV) cyanide complex *trans*- $[(\text{CNN})\text{Pt}(\text{CN})\text{I}_2]$ (**10**), the structure of which was elu-

(23) (a) Buil, M. L.; Esteruelas, M. A. *Organometallics* **1999**, *18*, 1798. (b) Hartbaum, C.; Mauz, E.; Roth, G.; Weissenbach, K.; Fischer, H. *Organometallics* **1999**, *18*, 2619, and references therein. (c) Kernbach, U.; Ramm, M.; Luger, P.; Fehlhammer, W. P. *Angew. Chem., Int. Ed. Engl.* **1996**, *35*, 310.

(24) Cardin, D. J.; Cetinkaya, B.; Lappert, M. F. *Chem. Rev.* **1972**, *72*, 545.

(25) Cardin, D. J.; Cetinkaya, B.; Cetinkaya, E.; Lappert, M. F.; Randall, E. W.; Rosenberg, E. *J. Chem. Soc., Dalton Trans.* **1973**, 1982.

(26) Michelin, R. A.; Bertani, R.; Mozzon, M.; Zanotto, L.; Benetollo, F.; Bombieri, G. *Organometallics* **1990**, *9*, 1449.

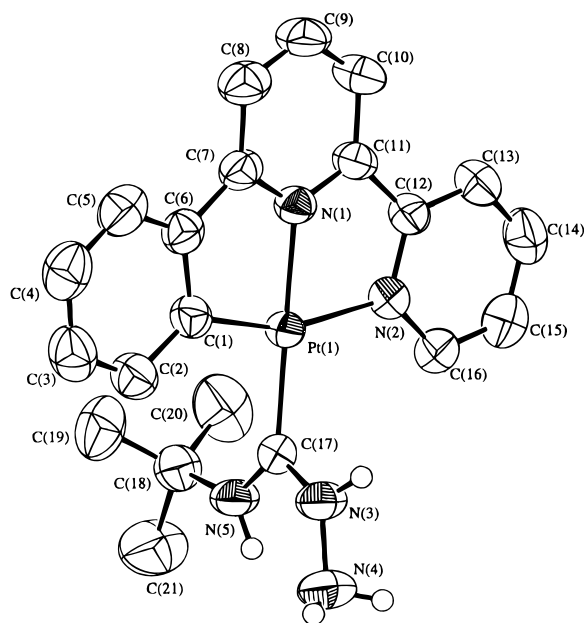


Figure 2. Perspective view of the cation in $3(\text{ClO}_4) \cdot 0.5\text{H}_2\text{O}$ (50% probability ellipsoids).

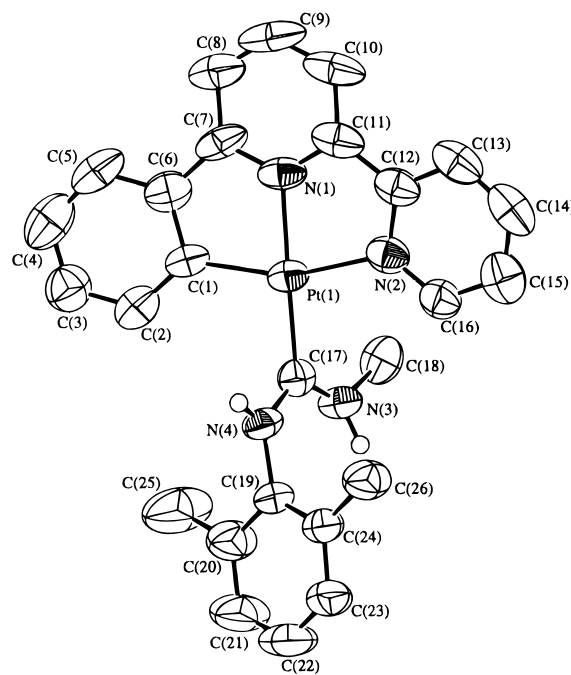


Figure 4. Perspective view of the cation in $6(\text{ClO}_4)$ (50% probability ellipsoids).

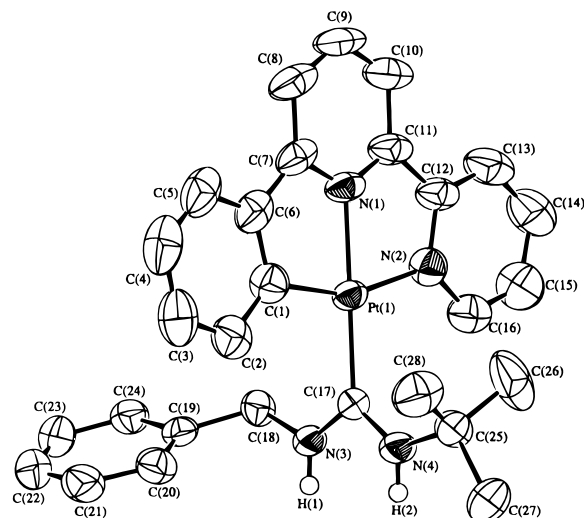


Figure 3. Perspective view of the cation in $4(\text{ClO}_4)$ (50% probability ellipsoids, positional disorder exists for C(1) and N(2)).

culated by X-ray crystallography (see below). Hence oxidation of the metal center and fragmentation of the diamino-carbene ligand are apparent. We found that heating an identical mixture at reflux resulted in formation of a number of unidentifiable species (**10** was not detected by IR or FAB-MS).

Crystal Structures. Structural determinations of $2(\text{ClO}_4) \cdot 0.5\text{H}_2\text{O}$, $3(\text{ClO}_4) \cdot 0.5\text{H}_2\text{O}$, $4(\text{ClO}_4)$, $6(\text{ClO}_4)$, and **10** have been performed (Figures 2–5); selected bond lengths and angles are listed in Table 2 (for $2(\text{ClO}_4) \cdot 0.5\text{H}_2\text{O}$, see Supporting Information). The molecular structure of each of the carbene complexes consists of a distorted square-planar environment at the platinum center, since the bite angle of the tridentate CNN ligand deviates substantially from 180° (C(1)–Pt(1)–N(2) for **2–4** and **6**: $159.6(3)^\circ$, $160.2(2)^\circ$, $159.2(2)^\circ$, and $159.0(3)^\circ$, respectively). The Pt(II)–C(carbene) distances (1.997(7), 1.992(4), 1.989(6), and 1.996(8) Å for **2–4** and **6**, respectively) are comparable to those in [Pt(CN)-

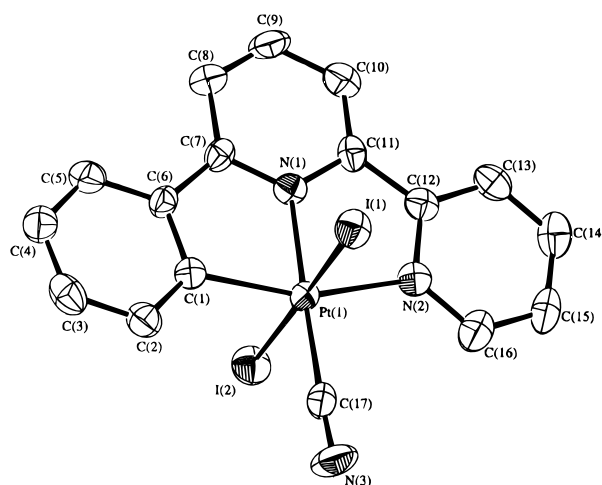


Figure 5. Perspective view of **10** (50% probability ellipsoids, positional disorder exists for C(1) and N(2)).

$(\text{C}_{10}\text{H}_{21}\text{N}_4)_6$ (1.97(1)–2.01(1) Å),⁷ *trans*-[Pt{C(NEt₂)(OC(O)Ph)}(PPh₃)I₂] (1.969(7) Å),²⁷ *trans*-[PtMe{C(NMe₂)Me}(PMe₂Ph)₂]PF₆ (2.079(13) Å),²⁸ [PtCl{η¹-Ar₂py}(μ-Cl)]₂ (1.951(9) Å without heteroatom stabilization, Ar₂py = 2,6-{2,4-(OC₆H₁₃)₂C₆H₃}₂C₆H₃N; carbene ligation at pyridyl C⁴),^{5b} and the Pt(IV) derivatives [PtCl₂Me(CH-NMe₂)(4,4'-t-Bu₂bpy)]Cl (1.991(21) Å)^{4a} and PtI₂{C(NHPr)-NH-3,4-(OMe)₂C₆H₂}₂ (2.039(6) and 2.037(6) Å).^{4b} All angles at the carbene carbon atoms in **2–4** and **6** approach 120° , which indicates *sp*² hybridization, but this does not necessarily amount to significant Pt–C(carbene) π bonding. Intriguingly, the Pt–C(aryl) [Pt(1)–C(1) for **2–4** and **6**: 2.001(8), 2.010(5), 2.068(5), and 2.033(9) Å, respectively] and Pt–C(carbene) distances differ by less than 0.05 Å. The short N–C(carbene) bond lengths (mean 1.332 Å) imply substantial *p*_π–*p*_π inter-

(27) Chen, J. T.; Tzeng, W. H.; Tsai, F. Y.; Cheng, M. C.; Wang, Y. *Organometallics* **1991**, *10*, 3954.

(28) Stepaniak, R. F.; Payne, N. C. *Inorg. Chem.* **1974**, *13*, 797.

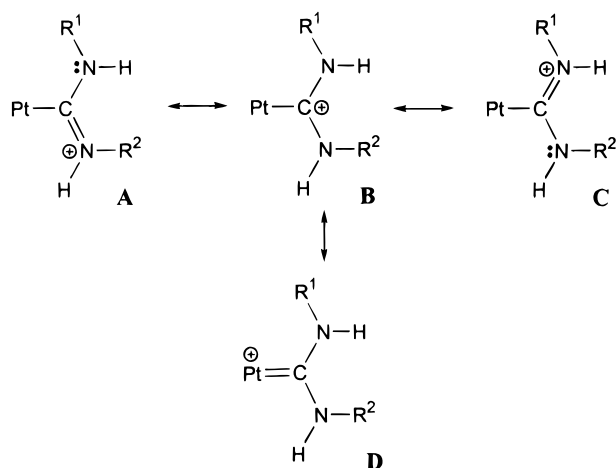


Figure 6. Resonance forms of the platinum(II) diamino-carbene interaction (CNN ligand omitted for clarity).

Table 2. Selected Bond Lengths (Å) and Angles (deg)

[(CNN)Pt{C(NH ^t Bu)(NHNH ₂)}]ClO ₄ ·0.5H ₂ O, 3 (ClO ₄)·0.5H ₂ O			
Pt(1)–N(1)	1.998(4)	Pt(1)–C(17)	1.992(4)
Pt(1)–N(2)	2.109(4)	C(17)–N(3)	1.319(6)
Pt(1)–C(1)	2.010(5)	C(17)–N(5)	1.327(6)
C(1)–Pt(1)–N(1)	81.4(2)	Pt(1)–C(17)–N(3)	116.2(3)
C(1)–Pt(1)–N(2)	160.2(2)	Pt(1)–C(17)–N(5)	129.2(4)
C(1)–Pt(1)–C(17)	98.0(2)	N(3)–C(17)–N(5)	114.6(4)
[(CNN)Pt{C(NH ^t Bu)(NHCH ₂ Ph)}]ClO ₄ , 4 (ClO ₄)			
Pt(1)–N(1)	1.999(5)	Pt(1)–C(17)	1.989(6)
Pt(1)–N(2)	2.087(6)	C(17)–N(3)	1.343(7)
Pt(1)–C(1)	2.068(5)	C(17)–N(4)	1.344(7)
C(1)–Pt(1)–N(1)	80.1(2)	Pt(1)–C(17)–N(3)	120.9(4)
C(1)–Pt(1)–N(2)	159.2(2)	Pt(1)–C(17)–N(4)	126.5(4)
C(1)–Pt(1)–C(17)	99.7(1)	N(3)–C(17)–N(4)	112.6(5)
[(CNN)Pt{C(NHAr')(NHMe)}]ClO ₄ , 6 (ClO ₄)			
Pt(1)–N(1)	2.006(6)	Pt(1)–C(17)	1.996(8)
Pt(1)–N(2)	2.110(8)	C(17)–N(3)	1.324(9)
Pt(1)–C(1)	2.033(9)	C(17)–N(4)	1.328(9)
C(1)–Pt(1)–N(1)	80.8(3)	Pt(1)–C(17)–N(3)	121.5(6)
C(1)–Pt(1)–N(2)	159.0(3)	Pt(1)–C(17)–N(4)	120.7(6)
C(1)–Pt(1)–C(17)	100.4(3)	N(3)–C(17)–N(4)	117.5(7)
<i>trans</i> -[(CNN)Pt(C≡N)I ₂], 10			
Pt(1)–N(1)	2.005(6)	Pt(1)–I(1)	2.6490(5)
Pt(1)–N(2)	2.102(7)	Pt(1)–I(2)	2.6718(6)
Pt(1)–C(1)	2.086(5)	Pt(1)–C(17)	1.988(9)
		C(17)–N(3)	1.14(1)
I(1)–Pt(1)–N(1)	88.9(1)	I(1)–Pt(1)–I(2)	177.89(2)
I(1)–Pt(1)–N(2)	91.6(2)	I(1)–Pt(1)–C(17)	89.7(2)
I(1)–Pt(1)–C(1)	87.8(2)	Pt(1)–C(17)–N(3)	177.4(7)

actions within the N–C(carbene)–N fragment, and this is clearly inferred from ¹H NMR spectroscopy. The resonance forms for Pt(II) diamino-carbene bonding are shown in Figure 6. Based on structural and NMR data, we suggest that forms **A** and **C** contribute noticeably more to the hybrid structure than form **D**. A recent experimental and theoretical study of platinum and palladium bis(diamino-carbene) complexes found little evidence for π bonding.²⁹

The diamino groups of the carbene moieties in **2–4** and **6** are orientated out of the [(CNN)Pt] plane to reduce steric repulsion. The *Z*, *E* arrangements of the amino substituents in **2**, **3**, and **6** are expected for these complexes, although the contrast between the *E* con-

formations for the *tert*-butyl groups in **2** and **3** and the *Z* arrangement for the 2,6-dimethylphenyl unit in **6** may be explained on steric grounds. The *Z*, *Z* configuration in **4** is therefore unusual. Close inspection of the crystal lattice reveals weak hydrogen bonds between the amino hydrogens and the perchlorate groups (N–H...O–Cl ca. 3.0 Å), which evidently stabilizes the lattice and compensates for the deviation away from the normal *Z*, *E* orientation. Weak π – π stacking interactions are apparent in the packing diagrams of **2–4** and **6** (range 3.5–3.6 Å). This has notable consequences for the emissive properties of these luminophores, as is discussed in the following section.

The platinum center in **10** adopts a distorted octahedral geometry with coordination of tridentate cyclometalated CNN, cyanide, and *trans*-diiodide ligands. The short C(17)–N(3) bond distance of 1.14(1) Å is consistent with a carbon–nitrogen triple bond. The Pt–C(17) bond length of 1.988(9) Å closely resembles the Pt–C(carbene) distances in this work (mean 1.994 Å). Since the cyanide ligand is a strong σ -donor and weak π -acid and minimal metal–cyanide π bonding is expected, this observation provides further support for the notion that the Pt–C(carbene) interaction in diamino-carbene complexes does not exhibit significant π character.

Absorption and Emission Spectroscopy. The UV–visible spectral data of complexes **1–10** in acetonitrile are listed in Table 3 (see Figure 7 for **3**). Like for previously described Pt(II) complexes,^{12,15,16,30} the moderately intense low-energy band with λ_{\max} in the range 386–401 nm is assigned to ¹MLCT (5d)Pt → π^* (CNN) transitions, while the shoulder at $\lambda_{\max} > 425$ nm is attributed to ³MLCT states. An increase in the electrophilicity of the metal center is expected to result in a blue-shift for these MLCT transitions. For example, the singlet MLCT absorptions for the cations **1–9** appear at higher energies than the neutral analogue [(CNN)PtCl] (420 nm in CH₃CN),¹⁵ while the UV–vis spectrum for the Pt(IV) derivative **10** reveals no absorptions at $\lambda_{\max} > 380$ nm.

All isocyanide and carbene complexes in this study are emissive in solution and solid states at room temperature (Tables 4 and 5, respectively). With reference to earlier work on cyclometalated Pt(II) derivatives,^{13,15,16} the structureless emissions of complexes **1–9** in CH₃CN at 298 K are assigned as ³MLCT in nature. Transformation of isocyanide ligands to diamino-carbene moieties results in red-shifts for the emission maxima from 528/533 nm (for **5** and **1**, respectively) to 542–558 nm (for **2–4** and **6–8**) (see Figure 8 for **1** and **2**). The emission maximum for the binuclear bridging bis(carbene) complex **9** (λ_{\max} 545 nm) falls within the range observed for the mononuclear counterparts. This suggests that the two [(CNN)Pt] moieties in **9** behave as discrete noninteracting fragments from a spectroscopic perspective, since Pt(II)–Pt(II) and/or ligand–ligand interactions would yield MMLCT emission at $\lambda_{\max} > 600$ nm.^{15,16} Lifetimes ranging from 0.18 and 0.30 μ s (for **3** and **6**, respectively) up to 2.64 and 3.50 (for **2** and **9**, respectively) μ s are detected. Self-quenching of the emissions are evident

(29) Green, J. C.; Scurr, R. G.; Arnold, P. L.; Cloke, F. G. N. *Chem. Commun.* **1997**, 1963.

(30) Houlding, V. H.; Miskowski, V. M. *Coord. Chem. Rev.* **1991**, *111*, 145.

Table 3. UV–Vis Absorption Data in Acetonitrile (carbene complexes: [(CNN)Pt{C(NHR¹)NHR²}]ClO₄)

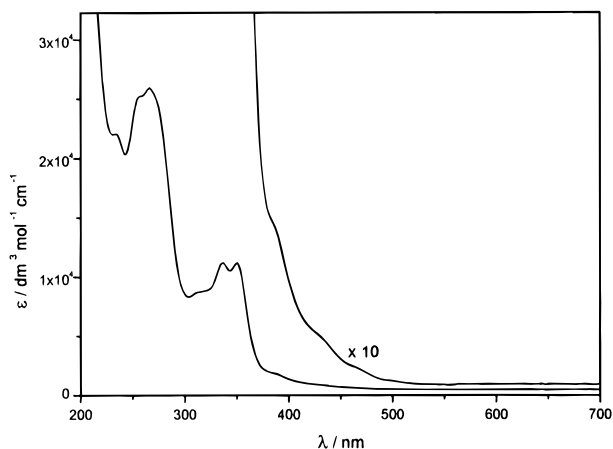
complex	λ_{\max}/nm ($\epsilon/\text{dm}^3 \text{ mol}^{-1} \text{ cm}^{-1}$)
[(CNN)Pt(C≡N ^t Bu)]ClO ₄ , 1 (ClO ₄)	250 (27800), 264 (26800), 333 (12800), 348 (12000), 398 (sh, 1000)
2 (ClO ₄): R ¹ = ^t Bu, R ² = Me	256 (27700), 269 (28800), 336 (12500), 350 (12700), 391 (1820), 435 (590), 469 (260)
3 (ClO ₄): R ¹ = ^t Bu, R ² = NH ₂	234 (22000), 258 (25200), 266 (26000), 337 (11200), 350 (11200), 387 (1800), 429 (500), 465 (230)
4 (ClO ₄): R ¹ = ^t Bu, R ² = CH ₂ Ph	257 (27800), 267 (28300), 317 (10400), 336 (12000), 350 (12100), 388 (1800), 430 (750), 462 (470)
[(CNN)Pt(C≡NAr ^r)]ClO ₄ , 5 (ClO ₄)	248 (31000), 266 (28000), 330 (12400), 350 (12000), 401 (sh, 1000)
6 (ClO ₄): R ¹ = Ar ^r , R ² = Me	234 (27500), 255 (27700), 266 (29000), 311 (9000), 336 (12500), 350 (12700), 389 (1650), 433 (600), 468 (300)
7 (ClO ₄): R ¹ = Ar ^r , R ² = NH ₂	234 (26500), 258 (25900), 267 (26900), 336 (10900), 350 (10600), 400 (1400), 470 (400)
8 (ClO ₄): R ¹ = Ar ^r , R ² = CH ₂ Ph	254 (26700), 266 (26000), 309 (9900), 320 (10400), 336 (10800), 350 (11000), 389 (1400), 430 (470), 466 (200)
[(CNN)Pt] ₂ μ -{C(NH ^t Bu)(NH(CH ₂) ₃) ₂ NMe}(ClO ₄) ₂ , 9 (ClO ₄) ₂	257 (19500), 266 (19600), 316 (7260), 351 (8280), 386 (1080), 430 (400)
<i>trans</i> -[(CNN)Pt(C≡N)] ₂ , 10	231 (34700), 260 (34000), 367 (7650)

Table 4. Emission Data in acetonitrile unless otherwise stated, (complex concentration = 5 × 10⁻⁵ M, carbene complexes: [(CNN)Pt{C(NHR¹)NHR²}]ClO₄)

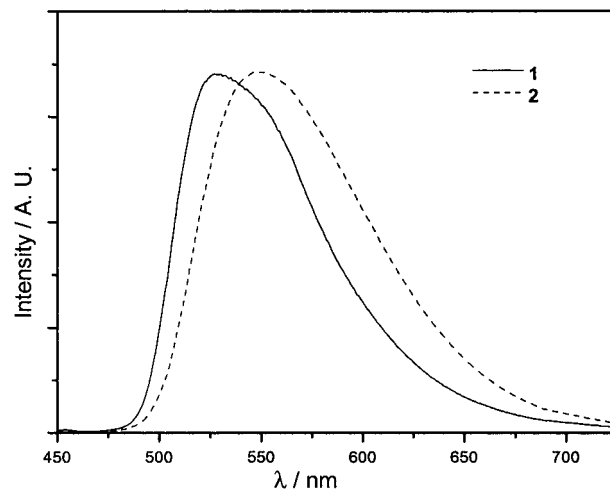
complex	298 K	77 K
	λ_{\max}/nm ; $\tau_0/\mu\text{s}$; ϕ_0	λ_{\max}/nm
[(CNN)Pt(C≡N ^t Bu)]ClO ₄ , 1 (ClO ₄)	533; 1.12; 0.11	505 (max), 538, 581 (sh) ^a
2 (ClO ₄): R ¹ = ^t Bu, R ² = Me	549; 2.64; 0.089	536 (max), 573, 625 (sh)
3 (ClO ₄): R ¹ = ^t Bu, R ² = NH ₂	550; 0.18; 0.011	538 (max), 576, 624 (sh)
4 (ClO ₄): R ¹ = ^t Bu, R ² = CH ₂ Ph	545; 1.17; 0.079	530 (max), 568, 612 (sh)
[(CNN)Pt(C≡NAr ^r)]ClO ₄ , 5 (ClO ₄)	528; 1.18; 0.13	519 (max), 554, 598 (sh)
6 (ClO ₄): R ¹ = Ar ^r , R ² = Me	548; 0.30; 0.025	525 (max), 562, 611 (sh)
7 (ClO ₄): R ¹ = Ar ^r , R ² = NH ₂	558; 0.56; 0.016	515 (max), 550, 600 (sh) ^a
8 (ClO ₄): R ¹ = Ar ^r , R ² = CH ₂ Ph	542; 1.14; 0.0025	532 (max), 570, 618 (sh)
[(CNN)Pt] ₂ μ -{C(NH ^t Bu)(NH(CH ₂) ₃) ₂ NMe}(ClO ₄) ₂ , 9 (ClO ₄) ₂	545; 3.50; 0.090	529 (max), 560, 610 (sh)

^a Measured in butyronitrile.**Table 5. Solid-State Emission Data (carbene complexes: [(CNN)Pt{C(NHR¹)NHR²}]ClO₄)**

complex	298 K	77 K
	λ_{\max}/nm ; $\tau_0/\mu\text{s}$	λ_{\max}/nm
[(CNN)Pt(C≡N ^t Bu)]ClO ₄ , 1 (ClO ₄)	579, 612 (sh); 2.60	547 (sh), 568 (max), 610 (sh)
2 (ClO ₄): R ¹ = ^t Bu, R ² = Me	572, 605 (sh); 1.76	555 (max), 599, 650 (sh)
3 (ClO ₄): R ¹ = ^t Bu, R ² = NH ₂	568, 604 (sh); 2.04	559 (max), 600, 652 (sh)
4 (ClO ₄): R ¹ = ^t Bu, R ² = CH ₂ Ph	563, 602 (sh); 1.69	560 (max), 603, 655 (sh)
[(CNN)Pt(C≡NAr ^r)]ClO ₄ , 5 (ClO ₄)	704; 0.42	781
6 (ClO ₄): R ¹ = Ar ^r , R ² = Me	570, 599 (sh); 3.04	561 (max), 603, 660 (sh)
7 (ClO ₄): R ¹ = Ar ^r , R ² = NH ₂	573; 1.72	556 (max), 598, 654 (sh)
8 (ClO ₄): R ¹ = Ar ^r , R ² = CH ₂ Ph	553, 595 (sh); 2.49	546 (max), 585, 635 (sh)
[(CNN)Pt] ₂ μ -{C(NH ^t Bu)(NH(CH ₂) ₃) ₂ NMe}(ClO ₄) ₂ , 9 (ClO ₄) ₂	568; 1.42	537 (max), 572, 627

**Figure 7.** UV–vis absorption spectra of **3** in acetonitrile at 298 K.

(e.g., $k_q = 5.6 \times 10^8$ and $1.8 \times 10^8 \text{ M}^{-1} \text{ s}^{-1}$ for **2** and **9**, respectively), where in each case a linear plot of $1/\tau$ versus complex concentration was obtained. Significantly, high emission quantum yields on the order of 0.1 are observed for the isocyanide complexes **1** and **5**.

**Figure 8.** Emission spectra of **1** and **2** in acetonitrile at 298 K (λ_{ex} 350 nm, normalized intensities).

This may be rationalized by the strong ligand field of $\text{RN}\equiv\text{C}$, which effects an increase in the energy of ligand-field excited states so that radiationless decay is less

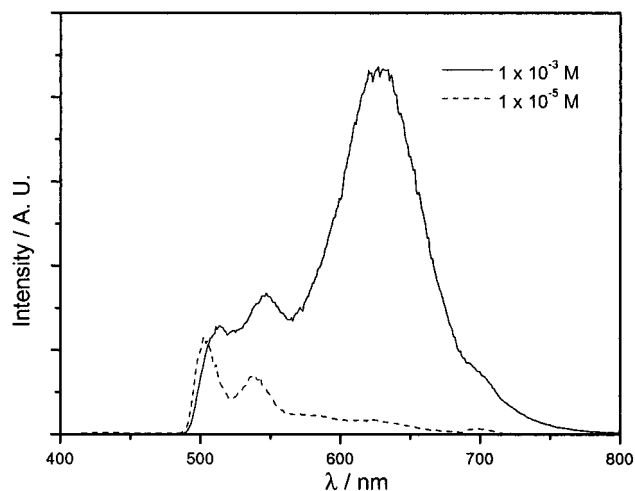


Figure 9. Emission spectra of **1** at different concentrations in butyronitrile at 77 K (λ_{ex} 350 nm).

prevalent. According to reports by Gray and Miskowski, the $^3\text{MLCT}$, ^3IC , and ^3dd states of Pt(II)–diimine complexes are very close in energy,³⁰ and nonradiative decay via low-energy d–d excited states has been proposed to be responsible for the low quantum yields of the $^3\text{MLCT}$ emission of $[\text{Pt}(\text{tpy})\text{Cl}]^+$ complexes.³¹ We also note that Pt(II) bpy and tpy complexes typically exhibit very weak emission (ϕ_0 on the order of 10^{-4} – 10^{-3}) in solution at room temperature,^{32,33} whereas derivatives bearing the cyclometalated 2-(2'-thienyl)pyridyl ligand can display large quantum yields of magnitude similar to **1** and **5**.^{34,35}

The frozen emissions of **1**–**9** at 77 K have been studied (Table 4). The 77 K emissions of **2**–**4** and **6**–**9** in acetonitrile are insensitive to the complex concentration in the range 10^{-6} – 10^{-3} M. Vibronically structured emission bands are detected at λ_{max} 515–538 nm which are blue-shifted from 298 K. The vibrational spacings of ca. 1200 cm^{-1} correspond to the skeletal stretching of the free HCNN ligand. The most intense vibronic component is $\nu' = 0$ to $\nu'' = 0$, indicating that these are $^3\text{MLCT}$ emissions. The concentration-dependent emissive behavior of **1** (Figure 9) and **5** in butyronitrile and acetonitrile, respectively, at 77 K has been investigated. A vibronic yellow emission at [in the order **1/5**] λ_{max} 505/519 nm (vibronic progression ca. 1220 cm^{-1}) is exhibited at low concentrations ($\sim 10^{-6}$ M). Dramatic changes in the band shape are seen upon increasing the complex concentration, where a new red emission centered at 627/730 nm develops at the expense of the yellow band. The UV–vis absorption spectra of **1** and **5** for concentrations below 10^{-3} M follow Beer's law and indicate the absence of ground-state oligomerization processes. For **1**, emission from solid-state phases in frozen solution is discounted because this occurs at λ_{max} 568 nm

(31) Bailey, J. A.; Hill, M. G.; Marsh, R. E.; Miskowski, V. M.; Schaefer, W. P.; Gray, H. B. *Inorg. Chem.* **1995**, *34*, 4591.

(32) Cummings, S. D.; Eisenberg, R. *J. Am. Chem. Soc.* **1996**, *118*, 1949.

(33) Aldridge, T. K.; Stacy, E. M.; McMillin, D. R. *Inorg. Chem.* **1994**, *33*, 722.

(34) (a) Maestri, M.; Sandrini, D.; Balzani, V.; Chassot, L.; Joliet, P.; von Zelewsky, A. *Chem. Phys. Lett.* **1985**, *122*, 375. (b) Kvam, P.-L.; Puzyk, M. V.; Cotlyr, V. S.; Balashev, K. P.; Songstad, J. *Acta Chem. Scand.* **1995**, *49*, 645.

(35) Lai, S. W.; Chan, M. C. W.; Cheung, K. K.; Peng, S. M.; Che, C. M. *Organometallics*, in press.

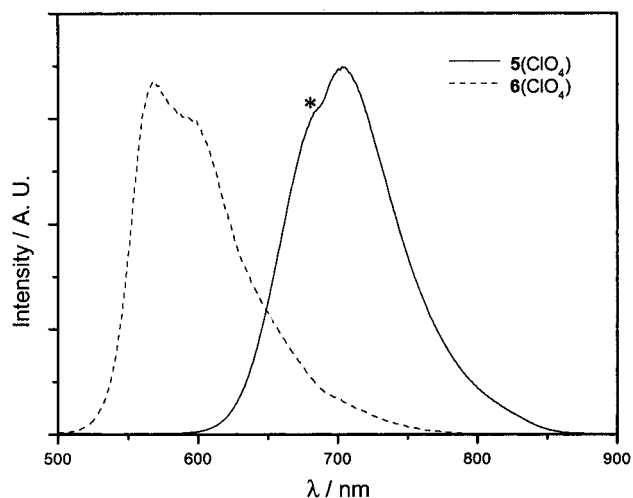


Figure 10. Solid-state emission spectra of **5**(ClO₄) and **6**(ClO₄) at 298 K (λ_{ex} = 350 nm, normalized intensities, asterisk denotes instrumental artifact).

at 77 K (Table 5). The 627 nm band for **1** is tentatively ascribed to excimeric intraligand emission arising from weak π -stacking interaction of the CNN ligand, by reference to previous studies on $[\text{Pt}(\text{tpy})\text{Cl}]^+$ (π – π excimeric emission at 650 nm) by Gray and co-workers.³¹ The shape and energy of the 730 nm band for **5** is very similar to the 740 nm glassy emission of $[\text{Pt}(\text{tpy})\text{Cl}]^+$ at 77 K and can be attributed to MMLCT excited states resulting from oligomerization of Pt(II) centers in glassy solutions.^{31,36}

The solid-state emissions of complexes **1**(ClO₄)–**9**(ClO₄)₂ [except **5**(ClO₄)] at 298 K show poorly resolved vibronic structures. They are red-shifted from solution to λ_{max} 553–579 nm with a shoulder at 595–612 nm [see Figure 10 for **6**(ClO₄)], while at 77 K a blue-shift is detected (Table 5). The emissions are tentatively assigned to $^3\text{MLCT}$ excited states with excimeric character due to weak CNN π – π interactions. As described in the previous section, stacking interactions are evident in the crystal lattice of these complexes (range 3.5–3.6 Å). Similar emissive behavior has been observed for related Pt(II)¹³ and transmetalated Au(III) species.³⁷ The purple color of **5**(ClO₄) in the solid state is striking and is accredited to the propensity for these square-planar Pt(II) species, like the established diimine relatives reported by Miskowski and Houlding,^{30,38} to undergo solid-state intermolecular stacking interactions which yield low-energy MMLCT transitions. At 298 K, microcrystalline samples of **5**(ClO₄) emit at λ_{max} 704 nm (Figure 10). Upon cooling to 77 K, the bandwidth of the emission decreases and the emission maximum red-shifts to 781 nm, which is remarkably low for MMLCT emissions of Pt(II) diimine solids. By comparison, the solid-state $^3\text{MMLCT}$ emission of $[\text{Pt}(\text{tpy})\text{Cl}]\text{ClO}_4$ at 298 K appears at λ_{max} 725 nm and blue-shifts to λ_{max} 695 nm at 77 K.³¹

(36) Yip, H. K.; Cheng, L. K.; Cheung, K. K.; Che, C. M. *J. Chem. Soc., Dalton Trans.* **1993**, 2933.

(37) Wong, K. H.; Cheung, K. K.; Chan, M. C. W.; Che, C. M. *Organometallics* **1998**, *17*, 3505.

(38) (38)(a) Miskowski, V. M.; Houlding, V. H. *Inorg. Chem.* **1989**, *28*, 1529. (b) Miskowski, V. M.; Houlding, V. H. *Inorg. Chem.* **1991**, *30*, 4446.

Concluding Remarks

This account has described the convenient and efficient synthesis of cyclometalated platinum(II) isocyanide and carbene complexes. The bidentate bis(carbene) moiety in complex **9** represents a novel class of bridging ligand which may gain prominence in multinuclear coordination chemistry. The crystal structures of the diamino-carbene derivatives as well as ^1H NMR data reflect π -delocalization throughout the N-C(carbene)-N fragment. Concurrently, the Pt-C(carbene) distances are only slightly shorter (<0.05 Å) than the Pt-C(aryl) contacts, and hence minimal π character in the Pt-C(carbene) interaction is proposed.

All complexes display photoluminescence in solution at room temperature. We suggest that the strong ligand field strengths of the isocyanide ligands, which decreases the electrophilicity of Pt(II) and destabilizes metal-centered transitions, have considerable impact upon the emissive behavior of this system. Hence the fluid emissions of the isocyanide derivatives **1** and **5** are

blue-shifted from that of the carbene species, while significantly higher emission quantum yields are displayed by **1** and **5**. In future work, incorporation of isocyanide ligands to improve the photophysical parameters of other classes of luminophores is anticipated. To the best of our knowledge, the 77 K solid-state emission of **5**(ClO₄) at λ_{max} 781 nm is the lowest reported MMLCT emission for square-planar platinum(II) diimine-type solids.^{30,38}

Acknowledgment. We are grateful for support from The University of Hong Kong and the Hong Kong Research Grants Council.

Supporting Information Available: Tables of crystal data, atomic coordinates, calculated coordinates, anisotropic displacement parameters, and bond lengths and angles for **2**(ClO₄)·0.5H₂O, **3**(ClO₄)·0.5H₂O, **4**(ClO₄), **6**(ClO₄), and **10**. This material is available free of charge via the Internet at <http://pubs.acs.org>.

OM990256H